



## UvA-DARE (Digital Academic Repository)

### Cardiac microvascular dysfunction

*Insights from COVID-19, myocardial infarction, and anthracycline-induced cardiotoxicity*

Jiang, Z.

#### Publication date

2026

[Link to publication](#)

#### Citation for published version (APA):

Jiang, Z. (2026). *Cardiac microvascular dysfunction: Insights from COVID-19, myocardial infarction, and anthracycline-induced cardiotoxicity*. [Thesis, fully internal, Universiteit van Amsterdam].

#### General rights

It is not permitted to download or to forward/distribute the text or part of it without the consent of the author(s) and/or copyright holder(s), other than for strictly personal, individual use, unless the work is under an open content license (like Creative Commons).

#### Disclaimer/Complaints regulations

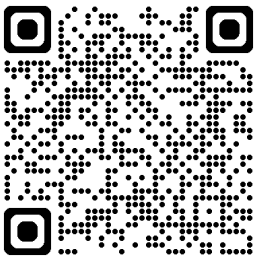
If you believe that digital publication of certain material infringes any of your rights or (privacy) interests, please let the Library know, stating your reasons. In case of a legitimate complaint, the Library will make the material inaccessible and/or remove it from the website. Please Ask the Library: <https://uba.uva.nl/en/contact>, or a letter to: Library of the University of Amsterdam, Secretariat, P.O. Box 19185, 1000 GD Amsterdam, The Netherlands. You will be contacted as soon as possible.

# Chapter 4

## Increased perivascular fibrosis and pro-fibrotic cellular transition in intramyocardial blood vessels in myocardial infarction patients

Zhu Jiang *MEng*, Giulia Sorrentino *BSc*, Suat Simsek *MD PhD*, Joris J.T.H. Roelofs *MD PhD*, Hans W.M. Niessen *MD PhD*, Paul A.J. Krijnen *PhD*

**Running title:** Perivascular and Cellular Fibrosis in MI



**Published in :**

*Journal of Molecular and Cellular Cardiology Plus*. Volume 10, December 2024,100275.

1

2

3

4

5

6

7

8

9

10

## Abstract

**Background and Objectives** Structural and functional changes in the intramyocardial microcirculation increase the risk of myocardial infarction (MI). This study investigated intramyocardial perivascular fibrosis and pro-fibrotic cellular transitions in deceased acute and subacute MI patients to explore their involvement in the pathogenesis of MI.

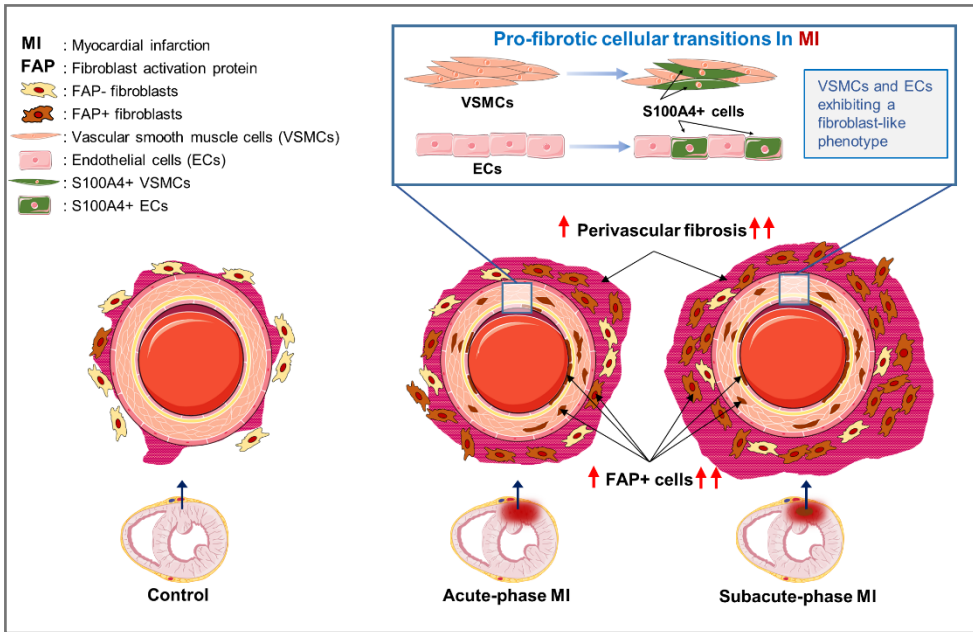
**Methods** Left ventricular tissue (LV) was obtained from the infarction area of autopsied patients with acute-phase MI (3-6 hours; n=24), subacute-phase MI (5-14 days; n=12), and noninfarcted controls (n=14). Perivascular fibrosis and fibroblast activation protein (FAP) expression were quantified using (immuno)histochemistry. Fibroblast-like transitioning of vascular smooth muscle cells (VSMC) and endothelial cells (EC) was quantified using immunofluorescent microscopy.

**Results** Perivascular fibrosis was elevated in acute-phase (77.69%) and subacute-phase (72.19%: border zone 95.18%: infarct core) MI patients ( $p<0.0001$ ) compared to controls (61.03%). FAP expression was higher in both acute-phase (1.46%) and subacute-phase (18.01%: border zone 5.67%: infarct core) compared to controls (0.46%) ( $p<0.05$ ). VSMC fibroblast-like cellular transition (SMA+S100A4+ vessels fraction) was higher in acute-phase (31.96%) and subacute-phase (21.90%: border zone; 37.25%: infarct core) MI compared to controls (8.95%) ( $p<0.05$ ). Similarly, EC fibroblast-like cellular transition (CD31+S100A4+ area fraction) was increased in acute-phase MI (10.14%) and subacute-phase MI (8.31%: border zone 10.15%: infarct core) compared to controls (2.67%) ( $p<0.05$ ).

**Conclusion** Increased perivascular fibrosis, fibroblast activation and vascular cellular transition in intramyocardial blood vessels of MI patients may contribute to MI development. Further increases of FAP expression and perivascular fibrosis, particularly in subacute-phase infarct cores, suggest MI itself exacerbates fibroblast activation and perivascular fibrosis, theoretically increasing reinfarction risk.

**Keywords:** Myocardial infarction; perivascular fibrosis; pro-fibrotic cellular transition; cardiovascular disease;

## Graphical Abstract



## Highlights:

- Intramyocardial perivascular fibrosis is increased in acute and subacute MI.
- Fibroblast-like transition of endothelial and smooth muscle cells are enhanced in MI.
- Profibrotic changes in the cardiac microvasculature may increase risk of MI.

## 1. Introduction

Myocardial infarction (MI) is characterized by the severe reduction or complete blockage of blood supply to a section of the heart muscle, resulting in irreversible ischemic tissue damage, that can lead to heart failure development, arrhythmias and death<sup>[1]</sup>. MI most often arises due to atherothrombotic events within the epicardial coronary arteries, which hence are the predominant focus of research into therapies and preventive measures of MI. However, structural and functional changes in the intramyocardial microcirculation, referred to as coronary microvascular dysfunction, are increasingly recognized to play an important role in myocardial ischemia and infarction<sup>[2]</sup>.

For instance, excessive accumulation of advanced glycation end-products was found in the intramyocardial vasculature of MI patients, indicative of vascular dysfunction [3]. In addition, MI patients exhibited thickened basement membranes of intramyocardial capillaries [4], as well as a decrease in perivascular adipose tissue (PVAT) around the larger intramyocardial blood vessel segments ((pre)arterioles)[5]. Interestingly, these structural and functional changes did not relate to the levels of stenosis and plaque instability of the epicardial coronary arteries and were already significant in infarctions of less than 6 hours old, suggesting they occurred prior to the onset of MI.

Intramyocardial arterioles, by their dilatational ability, play a crucial role in maintaining cardiac perfusion and oxygen supply [6]. Perivascular fibrosis, i.e. an increased amount of connective tissue around the vessels, might significantly limit this regulation of vascular tone, and thereby limit oxygen supply to the heart. Indeed, fibrotic remodelling of the microcirculation was shown to correlate with impaired coronary flow in patients with non-ischemic heart failure[7]. Moreover, MI initiates an increase in fibrotic activity, involving among others (myo)fibroblasts, to replace the lost myocardium with scar tissue, that in theory may also lead to perivascular fibrosis. However, how perivascular fibrosis, especially around (pre)arterioles, compares between patients that developed MI and age/sex-matched controls without heart failure, and how it evolves after MI, is unknown.

Fibroblast activation protein (FAP), a serine protease found on surface of, among others, activated fibroblasts, was shown to act as a key regulator of fibrotic responses in different organs, including the liver, lung and colon[8,9]. Moreover, FAP+ fibroblasts were found in areas of acute cardiac injury in heart tissue from MI patients and in the peri-infarct area 3 and 7 days post-MI and in the scar tissue 28 days post-MI[10] in rats, although a putative relation with the intramyocardial vasculature was not investigated.

Furthermore, under certain pathological conditions vascular cells, such as endothelial cells (ECs) and vascular smooth muscle cells (VSMCs), have been shown to transition toward fibroblast-like cells and to contribute to fibrosis. For instance, endothelial-to-mesenchymal transition (EndMT) was shown to contribute to cardiac fibrosis in mouse models of cardiac pressure overload and rejection[11] and to bleomycin-induced pulmonary fibrosis in mice[12]. While VSMCs with a fibroblast-like phenotype were shown to contribute to fibrous cap tissue of

atherosclerotic plaques<sup>[13]</sup> and vascular fibrosis<sup>[14]</sup>. However, the occurrence of these cellular transitions in the intramyocardial vasculature and their relation with perivascular fibrosis in MI patients is unknown.

In this study, we therefore investigated perivascular fibrosis, transition of VSMC and EC toward fibroblast-like cells and expression of FAP in the hearts of deceased patients at different time points after MI onset.

## 2. Materials and Methods

### 2.1 Patients

Transmural left ventricular heart tissues samples were obtained from 50 deceased patients who were referred to the Department of Pathology, Amsterdam UMC location VUmc, for clinical autopsy. The autopsies were performed within 24 hours after death. Of this cohort, 36 patients were diagnosed with recent left ventricular MI, showing macroscopical evidence of myocardial injury using nitro blue tetrazolium (NBT) staining. From the MI patients, samples taken from the NBT-identified infarction area were used. Fourteen age- and sex-matched patients, who died without any histopathological evidence of MI or cardiac ischemia, served as controls. The age of the infarctions was determined using microscopic criteria<sup>[15]</sup>. MI patients without microscopical accumulation of neutrophils in the vessels of the affected myocardium were diagnosed as acute-phase infarctions of 3-6 hours old; MI patients with microscopic granulation tissue in the affected myocardium were diagnosed as subacute-phase infarctions of 5-14 days old. After excision, the heart tissue was fixed overnight in formalin solution and subsequently embedded in paraffin. Part of the patients in this study have been used in a previous study<sup>[5]</sup>.

This research received approval from the ethics committee of Amsterdam UMC (Amsterdam, the Netherlands), and adhered to the principles outlined in the Declaration of Helsinki. The use of excised tissue at autopsy for research, after completion of diagnostics, was approved by the patients or their family. Patients or the public were not involved in the design, or conduct, or reporting, or dissemination plans of our research.

### 2.2 Immunohistochemistry

Heart tissue sections (4  $\mu\text{m}$ ) mounted on glass were utilized for immunohistochemically studies. The tissue sections underwent deparaffinization in

fresh xylene followed by rehydration through a graded series of alcohols (100% to 70%). To block endogenous peroxidase, the sections were treated with 0.3% H<sub>2</sub>O<sub>2</sub> for 20 min. For antigen retrieval, Tris-EDTA buffer (pH 9.0) was used at 98°C for 20 minutes. Blocking was performed with 10% goat serum for 10 minutes at room temperature (RT). All sections were incubated overnight at 4°C with a rabbit-anti-human FAP antibody (NBP2-66844; NOVUS, diluted 1:100). Following three TBS washes, the slides were incubated with envision secondary antibodies (Avantor, VWRKDPVR110HRP, undiluted) for 30 min at RT. Diaminobenzidine (DAB) (0.1mg/mL, Dako) was used for staining, followed by counterstaining with hematoxylin. For negative controls, some slides were stained without the primary antibody, showing no staining (results not displayed).

### **2.3 Elastin van Gieson Stain**

After deparaffinization and rehydration (as described in 2.2), the sections were stained with Lawson solution (Sigma-Aldrich, 1.00591.0500) for 30 min at RT. Sections was then washed in 100% alcohol and 96% alcohol for 10 sec respectively. After a wash in deionized water the sections were stained with 60% (v/v) hematoxylin for 10 min, subsequently washed with tap water for 10 sec, and then stained with Gieson solution for 10 min. The slides were then washed with tap water for 10 sec, dehydrated using incubation in increasing concentrations of alcohol (from 70% to 100%), and then covered with coverslips using Pertex.

### **2.4 Immunofluorescence**

After deparaffinization, rehydration and antigen retrieval (as described in 2.2), the sections were blocked with blocking solution for 10 min at RT. For a CD31 + SMA + either S100A4 or FAP triple staining, the sections were then incubated with mouse-anti-human CD31 antibody (Dako; M0823, 1:200 dilution), mouse-anti-human SMA antibody (Dako; M0851, 1:200 dilution) and rabbit-anti-human S100A4 antibody (abcam; ab197896, 1:2000 dilution) or rabbit-anti-human FAP antibody (NBP2-66844; NOVUS, diluted 1:100) overnight at 4°C. After three washes in PBS, the slides were incubated with Alexa Fluor 488-conjugated goat-anti-mouse IgG1 (Invitrogen, A21121, 1:500 dilution, for CD31) and Alexa Fluor 568-conjugated goat-anti-mouse IgG2a (Invitrogen, A21134, 1:500 dilution, for SMA) and Alexa Fluor 647 conjugated donkey-anti-rabbit IgG (Invitrogen, A31573, 1:500 dilution, for S100A4 or FAP) and with hoechst for 30 min at RT in the dark. In this study, slides were included that were stained without primary antibody and

without any antibodies as negative controls, and these were also used as reference to remove background staining during analysis.

## **2.5 (Immuno)histochemical and immunofluorescence quantification**

The slides used to analyse the expression of FAP in the myocardium and the perivascular fibrosis (stained by EVG) were scanned using a Philips scanner in bright field mode with Digital IntelliSite Pathology Solution v3.2 software. To quantify FAP expression, the FAP+ surface area of the myocardium was measured using Qupath-0.4.3 software and divided by the total myocardium surface area. For the quantification of perivascular fibrosis, the perivascular space of the larger branches of the intramyocardial vasculature was selected on scanned EVG-stained slides using Qupath-0.4.3 software. Herein, the surface areas of pink-stained connective tissue were measured and then divided by the total surface area of the perivascular space to obtain the individual percentage of perivascular fibrosis. These percentages were then averaged for each patient.

For the quantification of fibroblast-like cell transition of VSMCs and ECs immunofluorescent CD31+SMA+S100A4-stained slides were scanned using an Olympus VS200 slide scanner and Vectra Polaris scanner at 200x magnification under fluorescence mode. The scans were processed using Inform 2.6.0 software to remove the background fluorescence for analysis. The VSMC-to-mesenchymal transition was quantified by calculating the manually counted numbers of SMA+S100A4+ intramyocardial blood vessels as a percentage of the total numbers of SMA+ intramyocardial blood vessels within the tissues, using Qupath-0.4.3 software. The EC-to-mesenchymal transition was quantified by calculating the CD31+S100A4+ area as a percentage of the total CD31+ area, using Qupath-0.4.3 software.

In the heart tissue of subacute phase MI patients, immunoscore was performed separately in the infarct cores and border zones. Immunoscore was performed by two researchers (Z.J. and G.S) who were blinded to the clinical data.

## **2.6 Statistics**

Graphical representations were constructed using GraphPad Prism software, version 9, from San Diego, CA, USA. Statistical analyses of the data were performed utilizing SPSS software, version 26.0, from Armonk, NY, USA. Chi-Squared tests were employed to assess disparities in gender distribution. For comparing two

groups, t-tests were applied to Gaussian distributed data, while the Mann-Whitney U test was used for data non-Gaussian distribution. For comparing three or more groups, one-way analysis of variance (ANOVA) were applied to Gaussian distributed data, Kruskal-Wallis H test was used for data non-Gaussian distribution. P value below 0.05 was considered statistically significant. Gaussian distributed data were presented using mean  $\pm$  [standard deviation (SD)], while non-Gaussian distributed data were presented as median + [interquartile range (IQR)].

### 3. Results

#### 3.1 Patient characteristics

The clinical characteristics of the included patients are presented in **Table 1**. MI patients (n=36) were divided into two groups according to the age of infarction: acute phase MI (infarctions of 3-6 hours old; n=24) and subacute phase (infarctions of 5-14 days old; n=12). The mean  $\pm$  [SD] age of the controls, acute phase MI patients and subacute phase MI patients were  $56.1 \pm [17.1]$ ,  $62.13 \pm [18.60]$  and  $71.3 \pm [11.02]$  respectively. There were no significant differences in age and gender among the three groups.

#### 3.2 Perivascular fibrosis is increased in the myocardium of MI patients

Histological images of EVG-stained LV tissue of control patients (**Figure 1A**) and acute-phase MI patients (**Figure 1B**) are shown, depicting perivascular fibrosis around larger branches of the intramyocardial vasculature. **Figure 1C** shows a larger magnification of an intramyocardial blood vessel, highlighting pink-stained collagen fibres, black-stained elastic fibres and transparent adipose tissue. The mean  $\pm$  [SD] diameter ( $\mu\text{m}$ ) of the intramyocardial vessels selected for quantification was  $208.88 \pm [198.92]$ . The percentages of perivascular fibrosis were significantly increased both in acute-phase ( $77.69\% \pm [9.07\%]$ ,  $p < 0.0001$ ) and subacute-phase MI patients (infarct core ( $95.18\% \pm [4.41\%]$ ,  $p < 0.0001$ ) and border zone ( $72.19\% \pm [7.93\%]$ ,  $p < 0.05$ )) compared with controls ( $61.03\% \pm [12.60\%]$ ) (**Figure 1D**).

Within the infarct areas of subacute-phase MI patients, areas of granulation tissue (infarct cores) and areas of morphologically viable cardiomyocytes that surround the infarct cores (border zones) are present. As a strong fibrotic response is induced after MI, especially within the infarct cores to form scar tissue, we analysed the infarct cores and border zones also separately. In subacute-phase MI patients the

percentage of perivascular fibrosis in the infarct cores was significantly higher than the border zones ( $p < 0.0001$ ). The perivascular fibrosis did not differ significantly between the acute phase MI and border zones of subacute-phase MI patients.

We thus found increased intramyocardial perivascular fibrosis in patients with MI, already really acute after MI onset.

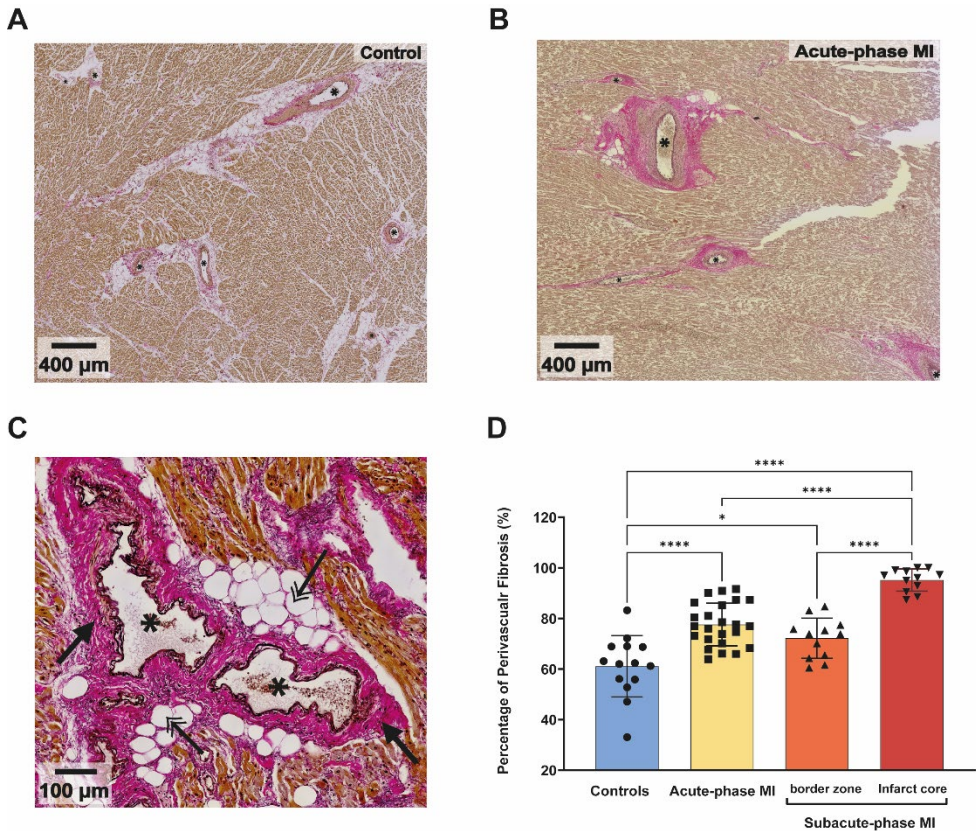


**Figure. 1** Intramyocardial perivascular fibrosis in MI patients.

Shown are examples of histological EVG staining of larger branches of the intramyocardial vasculature in the LV of control patients (A) and acute-phase MI patients (B), and a higher magnification of intramyocardial blood vessels in an acute-phase MI patient (C). The asterisks (\*) indicate blood vessels. The black arrows indicate pink-stained perivascular collagen fibres, and the black double arrows indicate spherical or ovoid-shaped transparent perivascular adipose tissue. Quantification of perivascular fibrosis in controls ( $n=14$ ), acute-phase MI ( $n=24$ ) and subacute-phase MI patients ( $n=12$ ) (D). Data are presented as mean [SD], each distinct point corresponds to the scores of individual patient: circles for controls, squares for acute-phase MI patients, triangles for the border zones and inverted triangles for the infarct cores of subacute-phase MI patients. The data followed a Gaussian distribution, one-way ANOVA was employed to assess the differences among the groups. A paired samples t-test was conducted to compare the data between the infarct core and border zone in subacute-phase MI. Error bars represent SD. Levels of significance were indicated as \* $p < 0.05$ , \*\*\*\* $p < 0.0001$ .

**Table 1. Clinical Characteristics of Patients in this study**

| Characteristic                         | Control<br>(n=14)  | MI <sup>a</sup><br>(n=36) |                          |
|--|--------------------|---------------------------|--------------------------|
|  |                    | Acute-phase<br>(n=24)     | Subacute-phase<br>(n=12) |
| <b>Age (Mean ± SD)<br/>(Range)</b>     | 56.1±17.1<br>29-81 | 62.1±18.6<br>26-95        | 71.3±11.0<br>48-95       |
| <b>Gender (n, %)</b>                   |                    |                           |                          |
| Female                                 | 7 (50%)            | 18 (75%)                  | 9 (75%)                  |
| Male                                   | 7 (50%)            | 6 (25%)                   | 3 (25%)                  |
| <b>Comorbidities/ Cardiac symptoms</b> |                    |                           |                          |
| Hypertension                           | 3 (21%)            | 2 (8%)                    | 1 (8%)                   |
| Lymphocytic Myocarditis                | 2 (14%)            | 4 (8%)                    | 1 (8%)                   |
| Arrhythmogenic cardiomyopathy          | 0 (0%)             | 1 (4%)                    | 0 (0%)                   |
| Diabetes mellitus                      | 0 (0%)             | 1 (4%)                    | 1 (8%)                   |
| <b>Cause of death</b>                  |                    |                           |                          |
| Myocardial Infarction                  | 0 (0%)             | 24 (100%)                 | 12 (100%)                |
| Pneumonia                              | 3 (21%)            | 0 (0%)                    | 0 (0%)                   |
| Aspiration                             | 1 (7%)             | 0 (0%)                    | 0 (0%)                   |
| Intoxication                           | 1 (7%)             | 0 (0%)                    | 0 (0%)                   |
| Viral encephalitis                     | 1 (7%)             | 0 (0%)                    | 0 (0%)                   |
| Menigo-encephalitis                    | 1 (7%)             | 0 (0%)                    | 0 (0%)                   |
| Cerebrovascular accident               | 4 (28%)            | 0 (0%)                    | 0 (0%)                   |
| Unknown cause of death                 | 3 (21%)            | 0 (0%)                    | 0 (0%)                   |

a: MI indicates patients with myocardial infarction. Control indicates patients died of other cause not related to MI. Chi-Squared test was employed to assess disparities in gender distribution. One-way ANOVA was applied to assess age difference among the controls, acute-phase MI and subacute-phase MI groups. There were no significant differences in age and gender among the three groups.

### 3.3 FAP expression is increased in the myocardium of MI patients

As the observed increase in perivascular fibrosis in MI patients may relate to increased fibroblast activity, we explored the expression of FAP in the myocardium of MI patients. In control patients only very limited FAP<sup>+</sup> cells were observed. In MI patients an increase in FAP expression was observed, which was present predominantly around intramyocardial blood vessels (**Figure 2A and B**). In subacute-phase MI patients, extensive perivascular FAP expression was observed in the border zones and in the infarct cores, where abundant FAP expression was present also in the granulation tissue (**Figure 2B**).

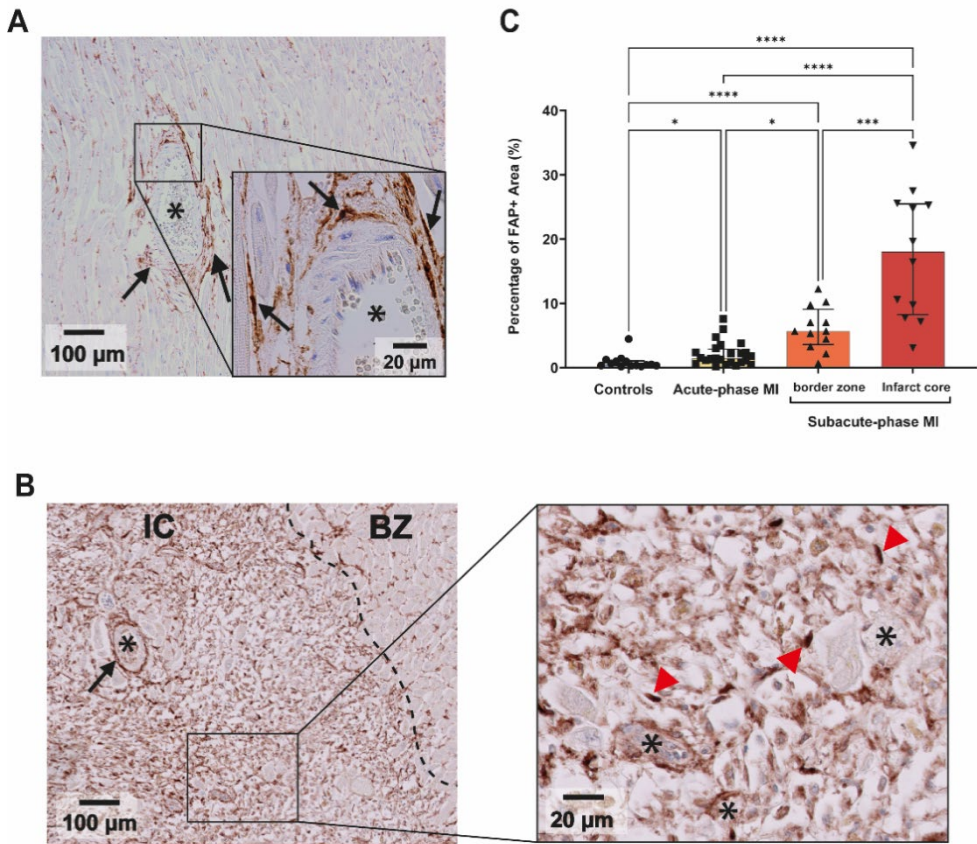


**Figure. 2 FAP expression in the myocardium of MI patients.**

Shown are examples of immunohistochemical FAP staining in the myocardium of acute-phase (**A**) and sub-acute-phase (**B**) MI patients. Asterisks (\*) indicate blood vessels; black arrows indicate perivascular FAP staining and red arrow-heads indicate FAP staining in the granulation tissue; IC and BZ indicate infarct cores and border zones respectively; Quantification of FAP expression in acute-phase and subacute-phase MI patients. Data are presented as median [IQR] in the graph, each distinct point corresponds to the scores of individual patient: controls (n=14; circles), acute-phase MI patients (n=24; squares) and subacute-phase MI patients (n=12; triangles for border zones, inverted triangles for infarct cores). A Kruskal-Wallis H test was used for statistical comparisons, due to the non-Gaussian distribution; a Wilcoxon matched-paired signed rank test was conducted to evaluate differences between the infarct core and border zone in subacute-phase MI. Error bars represent IQR. Levels of significance were indicated as \* $p < 0.05$ , \*\*\* $p < 0.001$ , \*\*\*\* $p < 0.0001$ .

Moreover, both in acute and subacute-phase MI, a limited number of blood vessels showed FAP expression also in endothelial cells and smooth muscle cells (**Figure 3A-C**). Colocalization of FAP with CD31 (biomarker of ECs) and with SMA (biomarker of VSMCs) using immunofluorescent microscopy confirmed the FAP expression in vascular cells (**Figure 3D**). The FAP+ area in the heart tissue of acute-phase MI patients (1.46% [0.79%-2.88%]) was a significant 3.2-fold higher than in

control patients (0.46% [0.30%-1.05%],  $p < 0.05$ ) (**Figure 2C**). In subacute-phase MI patients the FAP+ area in the infarct cores (18.01% [8.24%-25.48%]) was a significant 3.2-fold higher than that in the border zones (5.67% [3.60%-9.08%],  $p < 0.001$ ) (**Figure 2C**). Furthermore, the FAP+ areas in both the infarct core and border zone of subacute-phase MI patients were significantly higher than those in acute phase MI patients ( $p < 0.0001$  and  $p < 0.05$  respectively) and control patients ( $p < 0.0001$  and  $p < 0.0001$  respectively) (**Figure 2C**).

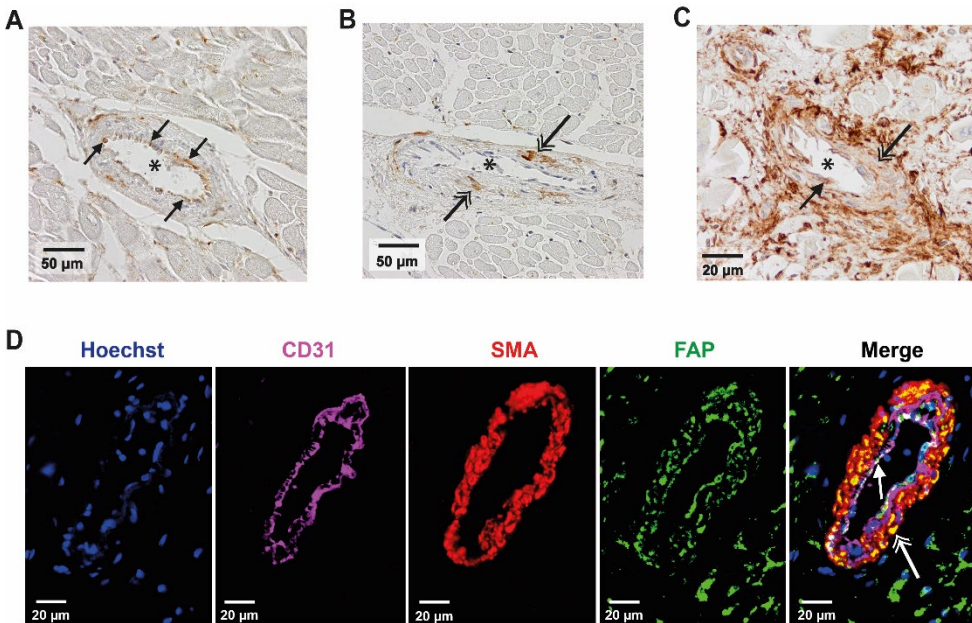


**Figure. 3 FAP expression in intramyocardial vascular cells of MI patients.**

Shown are examples of immunohistochemical staining for FAP, highlighting its expression in vascular cells in acute-phase (A and B) and sub-acute-phase (C) MI patients. Asterisks (\*) indicate blood vessels; black arrows indicate FAP-positive endothelial cells (A and C); black double arrows indicate vascular smooth muscle cells (B and C). Panel (D) displays an example of immunofluorescent staining for CD31 (purple), SMA (red) and FAP (green) in the myocardium of an acute-phase MI patient. Nuclei were stained with Hoechst (blue). Colocalization of CD31+FAP (white) in the endothelial layer is indicated in the merged image (white arrow), while colocalization of SMA+FAP (yellow) in the smooth muscle layer is shown (white double arrow).

We thus found increased FAP expression predominantly around intramyocardial blood vessels in the acute-phase infarcted heart, indicative of activated fibroblasts, that increased further in the subacute phase.

### 3.4 VSMC- and EC to mesenchymal transitions are increased in intramyocardial blood vessels in MI patients

Next, we analysed putative involvement of vascular cell transition toward fibroblast-like cells in the observed increase in perivascular fibrosis in MI patients. Firstly, the percentage of intramyocardial blood vessels wherein the fibroblast marker S100A4 was found in medial SMA+ VSMCs was quantified using immunofluorescent microscopy (**Figure 4A and C**). As SMA and S100A4 can be present also in myofibroblasts, only blood vessels wherein S100A4 was clearly present in the medial VSMC layer were counted as S100A4+SMA+ blood vessels (**Figure 4A and C**). In acute-phase (31.96% [24.44%-45.40%];  $p < 0.0001$ ) and subacute phase MI patients (infarct core (37.25% [20.34% - 44.00%]);  $p < 0.0001$ , and border zone (21.90% [10.28% -31.45%]);  $p < 0.05$ ) the fractions of SMA+S100A4+ intramyocardial blood vessels were significantly increased compared with controls (8.95% [8.05%-16.01%]) (**Figure 5A**). In subacute MI patients the fraction of SMA+S100A4+ blood vessels in the infarct core were a significant 1.7-fold higher than the border zone ( $p < 0.0001$ ; **Figure 5A**). The SMA+S100A4+ intramyocardial blood vessel fraction in the border zone of patients with subacute phase MI was slightly lower than that of patients with acute phase MI ( $p < 0.05$ ). There was no significant difference in the total number of SMA+ blood vessels per  $\text{cm}^2$  in the LV between the controls and the MI patients (not shown).

Secondly, we quantified the occurrence of EC to mesenchymal transition (EndMT). We observed expression of the fibroblast marker S100A4 in CD31+ ECs in both larger intramyocardial blood vessels as well as capillaries (**Figure 4B and C**). Hence, to quantify EndMT, the percentage of the CD31+ area wherein S100A4 was also found (CD31+S100A4+) was determined using immunofluorescence microscopy. There was a significant increase of EndMT in both acute-phase (10.14% [8.23%-14.61%];  $p < 0.0001$ ) and subacute-phase MI patients (infarct core (10.15% [6.77%-17.45%];  $p < 0.01$ , and border zone (8.31% [7.05%-11.40%];  $p < 0.05$ ) compared with the controls (2.67% [2.08%-5.94%]) (**Figure 5B**). A small but significant increase in EndMT was observed in the infarct core compared to border zone in subacute-phase MI patients ( $p < 0.05$ ), while there was no significant difference between acute-phase and subacute-phase MI patients (**Figure 5B**).

Therefore, mesenchymal transition of VSMC and EC was increased in the infarcted heart, already really acute after MI.

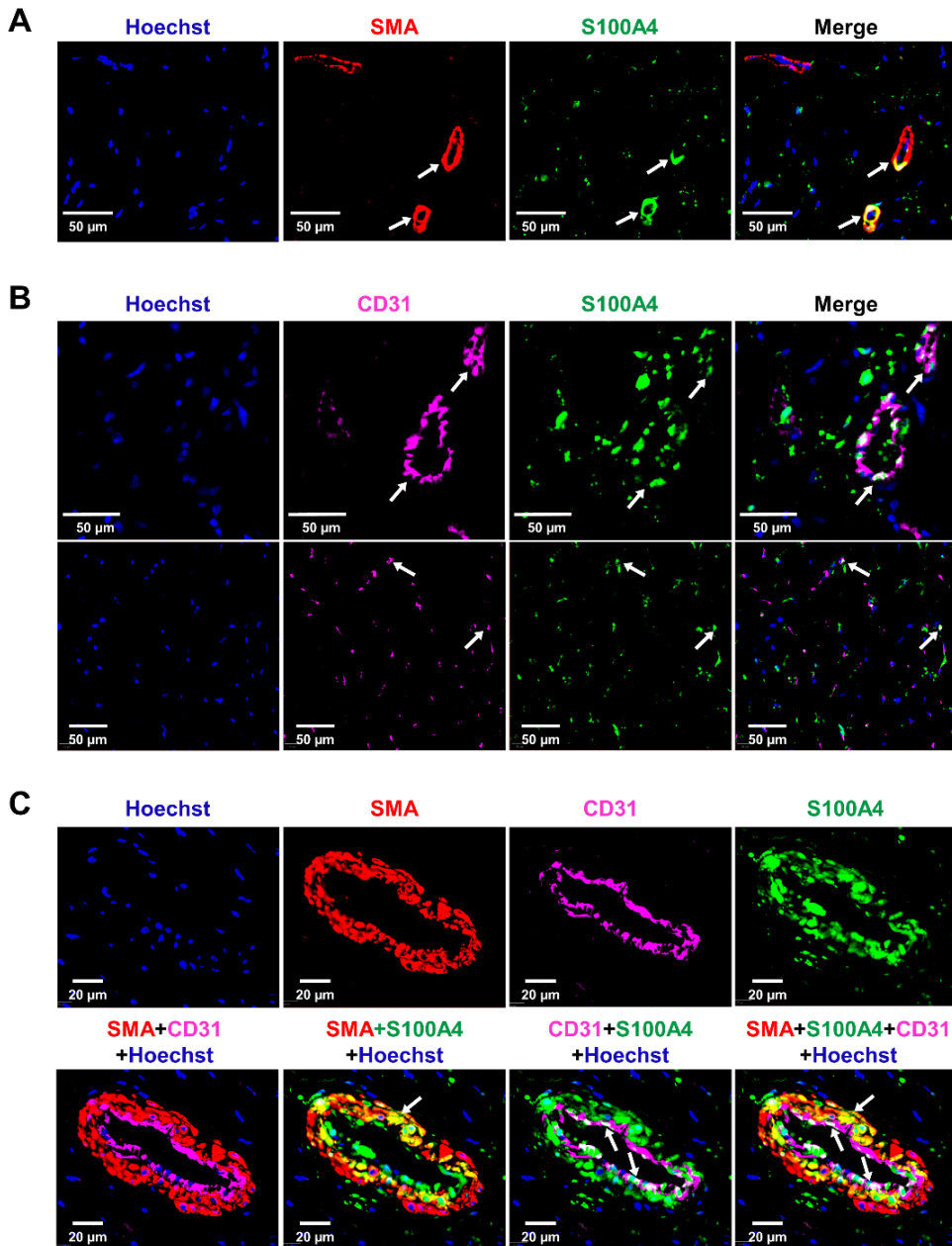


**Figure. 4 Pro-fibrotic cellular transition in intramyocardial blood vessels in MI patients.**

(A) Example of immunofluorescent staining for SMA (red), S100A4 (green) in the myocardium of an acute-phase MI patient. Nuclei were stained with Hoechst (blue). Colocalisation of SMA+S100A4 in the smooth muscle layer, indicating the VSMC-to-mesenchymal transition, is shown in the merged image (yellow). (B) Examples of immunofluorescent staining for CD31 (magenta), S100A4 (green) in the myocardium of an acute-phase MI patient (top row: arterioles; bottom row: capillaries). Nuclei were stained with Hoechst (blue). Colocalisation of

CD31+S100A4 in the endothelial layer, indicating endothelial-to-mesenchymal transition, is shown in the merged image (white). (C) Larger magnified example of immunofluorescent staining for SMA (red), CD31 (magenta), S100A4 (green) in the myocardium of an acute-phase MI patient (top row). Nuclei were stained with Hoechst (blue). Colocalization of SMA+S100A4 (yellow) and CD31+S100A4.

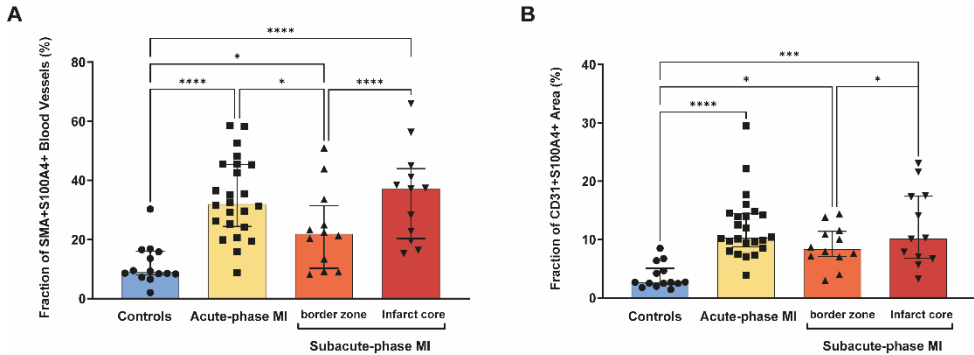


**Figure. 5 Quantification of pro-fibrotic vascular cellular transition in MI patients.**

Quantification of fibroblast-like transitioning of SMA+S100A4+ vascular smooth muscle cells (A) and CD31+S100A4+ endothelial cells (B) in controls (n=14), acute-phase (n=24) and subacute-phase MI (n=12) patients. Data are presented as median [IQR] in the graph, each distinct point corresponds to the scores of individual patient: circles for controls, squares for acute-phase MI patients, triangles for the border zones and inverted triangles for the infarct cores of subacute-phase MI patients. A Kruskal-Wallis H test was used for statistical comparisons, due to the non-Gaussian distribution; a Wilcoxon matched-paired signed rank test was conducted to evaluate differences between the infarct core and border zone in subacute-phase MI. Error bars represent IQR. Levels of significance were indicated as \* $p < 0.05$ , \*\*\* $p < 0.001$ , \*\*\*\* $p < 0.0001$ .

### 3.5 No gender differences in perivascular fibrosis, FAP expression and VSMC- and EC to mesenchymal transitions in MI patients.

As literature indicates that fibrotic responses may differ between men and women [16], we analysed putative differences in the extent of perivascular fibrosis, FAP expression and mesenchymal transitions between males and females. However, we found no significant differences in perivascular fibrosis (Figure 6A), FAP expression (Figure 6B), as well as fractions of SMA+S100A4+ intramyocardial blood vessels (Figure 6C) and the CD31+S100A4+ area (Figure 6D) between male and female patients of the control and MI groups.

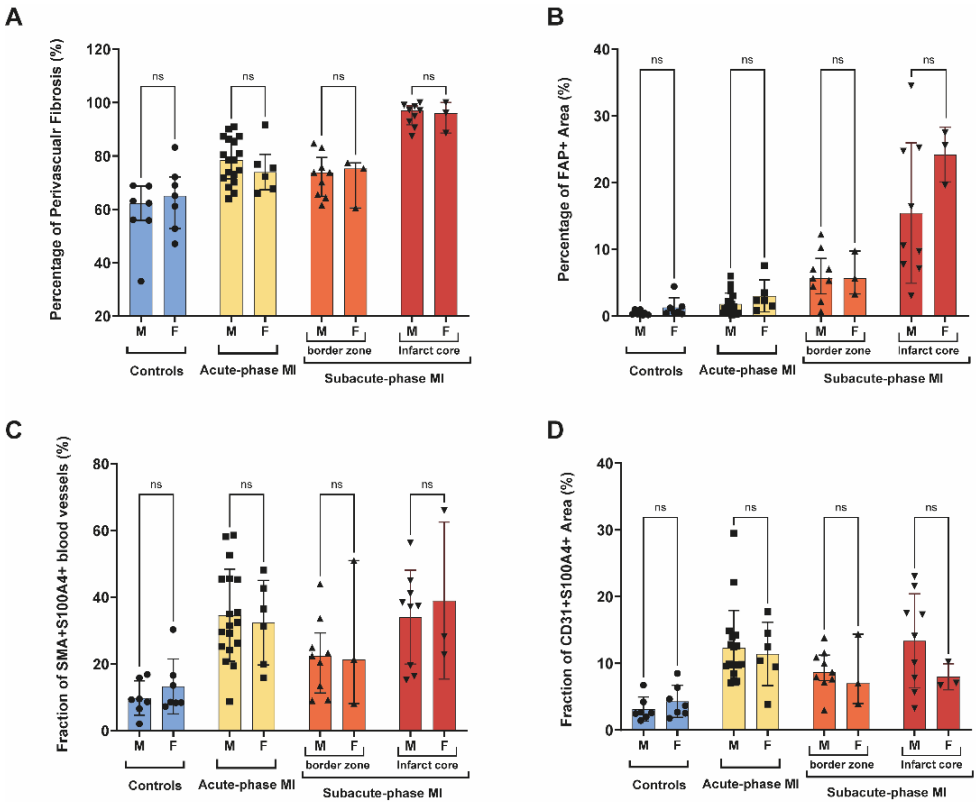


**Figure. 6 Gender-specific quantification of intramyocardial perivascular fibrosis, FAP expression and pro-fibrotic vascular cellular transition in MI patients.**

Shown are the quantifications of intramyocardial perivascular fibrosis (A), FAP expression (B), fibroblast-like transitioning of SMA+S100A4+ vascular smooth muscle cells (C) and CD31+S100A4+ endothelial cells (D) in male (M) versus female (F) controls (n=14), acute-phase (n=24) and subacute-phase MI (n=12) patients. Data are presented as median [IQR] in the graph. Each distinct point corresponds to the scores of individual patient: circles for controls, squares for acute-phase MI patients, triangles for the border zones and inverted triangles for the infarct cores of subacute-phase MI patients. A Mann-Whitney U test was used for statistical comparisons; Error bars represent IQR, ns indicated no statistic difference.

## 4. Discussion

In this study, we have analysed intramyocardial perivascular fibrosis, expression of FAP, and mesenchymal transition of vascular cells in the hearts of patients who died within 3-6 hours (acute phase) or 5-14 days (subacute phase) after MI. We found increased perivascular fibrosis and FAP expression, as well as an increased occurrence of VSMCs and ECs exhibiting a fibroblast-like phenotype, compared to age and sex-matched control patients. These profibrotic changes in the intramyocardial vasculature were significant already in acute phase MI. A further increase in especially perivascular fibrosis and FAP expression was observed in the infarct cores of subacute phase MI patients.

Perivascular fibrosis typically arises from factors such as enduring inflammation, endothelial dysfunction and mechanical stress, and generally is a prolonged process. In animal models the development of perivascular fibrosis in response to different stimuli spans days to weeks, even in *in vitro* models<sup>[17,18]</sup>. Moreover, the transition of animal and human ECs and VSMCs toward fibroblast like cells *in vitro* in response to different stimuli has been shown to take at least days to accomplish<sup>[19]</sup>. Given that the acute-phase MI patients in our study died within 3-6 hours following onset, it is thus likely that the observed accumulation of perivascular fibrotic tissue and phenotypic switching of vascular cells commenced prior to the onset of MI. This is in line with our previously observed AGEs accumulation, basement membrane thickening and PVAT loss in the intramyocardial vasculature in acute-phase MI patients<sup>[3]</sup> and potentially points to a pre-existing structurally and functionally changed coronary microvasculature in patients who develop MI.

Perivascular fibrosis can negatively affect vascular function in multiple ways. The increase in perivascular extracellular matrix (ECM) volume can lead to increased vascular stiffness and physically hinder vasodilation<sup>[20]</sup>. Moreover, perivascular fibrosis may reduce the contact of vasoactive factors, such as neuropeptides and adipokines released from perivascular nerves and PVAT, with the media and intima, thereby limiting the regulation of cardiac microvascular tension<sup>[5,21]</sup>. The decrease in intramyocardial PVAT we have observed before in acute-phase MI patients may further contribute to this decreased regulatory capacity<sup>[5]</sup>. Given the important role of (pre)arterioles in maintaining cardiac perfusion<sup>[6]</sup> and the negative effects of perivascular fibrosis on vascular function and coronary perfusion in patients with non-ischemic heart failure<sup>[7]</sup>, the increased perivascular fibrosis in the hearts of acute-phase MI patients may be a crucial contributor to the development of MI.

Furthermore, we found further elevation of perivascular fibrosis in the infarct cores of subacute-phase MI patients, where fibrotic tissue occupied on average over 95% of the adventitial space. As part of the post-infarct healing process, (myo)fibroblasts in the infarct core are activated to produce ECM proteins, such as collagen, for scar tissue formation<sup>[22,23]</sup>. Our finding of extensive FAP expression in the infarct cores of subacute-phase MI patients underscores this process. This indicates that the infarct-induced profibrotic activity in the infarct core exacerbates perivascular fibrosis in newly formed blood vessels, which may further restrict coronary vascular function and thereby contribute towards perfusion defects and reinfarction.

The increase in FAP expression, predominantly around the intramyocardial blood vessels of acute- and subacute-phase MI patients, points to increased activity of perivascular fibroblasts. Increased FAP expression levels were previously observed in activated cardiac fibroblasts in patients with ischemic and non-ischemic heart failure<sup>[10,24]</sup> and were found to correlate with key fibrosis markers<sup>[24]</sup>. Although these studies did not differentiate between interstitial and perivascular fibroblasts, they underscore a central role for FAP+ fibroblasts in cardiac fibrosis. Moreover, a recent study in mice with angiotensin II and phenylephrine-induced cardiac injury and fibrosis, showed that adoptive transfer of chimeric antigen receptor (CAR)-T cells targeted against FAP, significantly reduced cardiac fibrosis<sup>[25]</sup>. Our study thus points to involvement of activated FAP+ fibroblasts in the exacerbated perivascular fibrosis in MI patients.

In addition, we found increased transition of VSMCs and ECs towards a fibroblast-like phenotype in MI patients. It has been shown in coronary and aortic atherosclerotic plaques in humans and mice that fibroblast-like transitioning of both ECs and VSMCs occurs and that these fibroblast-like cells exhibit gene expression distinct from ECs and VSMCs, showing induced expression of proteins involved in ECM structure and regulation, such as collagens, fibronectins and metalloproteinases (MMPs) that shape the intraplaque fibrotic cap<sup>[26,27]</sup>. However, ECs and VSMCs may contribute to perivascular fibrosis also. Exclusive overexpression of oxidative stress associated protein p22phox in VSMCs resulted in aortic perivascular fibrosis and stiffening in mice<sup>[28]</sup>. While EndMT was shown to contribute to perivascular and cardiac fibrosis in diabetic mice<sup>[19]</sup> and in mice with pressure overload-induced cardiac fibrosis<sup>[11]</sup>. These studies highlight the potential involvement of ECs and VSMCs in perivascular fibrosis and point to a possible role of the increased fibroblast-like transitioning of these cells in the

observed intramyocardial perivascular fibrosis in MI patients we observed in the current study. This is in line with the presence of FAP we found in cardiac microvascular ECs and VSMCs in MI patients. Lastly, EndMT has also been shown to play a role in angiogenesis<sup>[29]</sup>. This might partly explain the large extent of phenotypic switching of vascular cells within the infarct cores of subacute-phase MI patients, wherein angiogenesis is predominant.

We found no differences in perivascular fibrosis and profibrotic cellular transitions between males and females in none of the groups. Previous studies indicate that especially premenopausal women are protected against severe forms of organ fibrotic responses, including in the heart, which may be related to sex hormones such as estrogen<sup>[16,30]</sup>. This protective effect is lost in postmenopausal women. Notably, the average age of the female patients in all groups was above 60, indicating that the majority of included female patients likely were postmenopausal. This may have reduced putative gender-related variability in the observed outcomes in our study.

One notable limitation of this study is its reliance on post-mortem tissue samples. Although perivascular fibrosis around the intramyocardial vasculature cannot be quantified accurately in living patients, the use heart tissue from deceased MI patients might introduce bias compared to living MI patients. Moreover, due to limited availability, data on cardiac function and perfusion could not be included in this study, preventing the analysis of putative relations between these clinical data and perivascular fibrosis and vascular cellular transitions in our patients. Lastly, the relatively small sample size, particularly for the subacute-phase MI group (n=12), may restrict the generalizability of the findings. Additionally, this small patient number as well as the imbalance in gender representation across groups also limited the power of gender-specific differences assessment. Future studies should aim to include larger cohorts with balanced gender representation and premenopausal women, along with prospectively record heart function and perfusion data to validate and extend these findings in a clinical setting.

In conclusion, we found increased intramyocardial perivascular fibrosis in MI patients that likely predates MI development and that progressed with infarct age, especially in the infarct cores, which may predispose to perfusion defects and reinfarction. Increased (peri)vascular fibroblast activity and pro-fibrotic vascular cell transitions may underlie this perivascular fibrosis and may provide potential

therapeutic targets for the prevention of adverse cardiac remodelling. Targeting (peri)vascular pro-fibrotic processes and vascular remodelling may hold promise for improving MI outcomes and reducing the risk of reinfarction.

### **Acknowledgments of grant support:**

This work was supported by the China Scholarship Council (Beijing, China, grant number 202008320278 to ZJ);

### **Author contributions**

**Zhu Jiang:** Methodology; Formal analysis; Data curation; Visualization; Writing - original draft; **Giulia Sorrentino:** Visualization; Formal analysis; Data curation; Writing - review; **Suat Simsek:** Resources; Methodology; Writing - review; **Joris J.T.H. Roelofs:** writing – review; **Hans W.M. Niessen:** Resources; Project administration; Conceptualization; Funding acquisition; Methodology; Supervision; Writing - review & editing; **Paul A.J. Krijnen:** Resources; Project administration; Conceptualization; Funding acquisition; Methodology; Supervision; Writing - review & editing;

### **Competing Interest**

The authors declare that they have no conflict of interest.

### **Disclosure**

None

## References

- [1]. Ojha N, Dharmoon AS. Myocardial Infarction. In: *StatPearls*. Treasure Island (FL): StatPearls Publishing Copyright © 2023, StatPearls Publishing LLC.; 2023.
- [2]. Del Buono MG, Montone RA, Camilli M, Carbone S, Narula J, Lavie CJ, Niccoli G, Crea F. Coronary microvascular dysfunction across the spectrum of cardiovascular diseases: JACC state-of-the-art review. *Journal of the American College of Cardiology*. 2021;78:1352–1371.
- [3]. Baidoshvili A, Krijnen PA, Kupreishvili K, Ciurana C, Bleeker W, Nijmeijer R, Visser CA, Visser FC, Meijer CJ, Stooker W, et al. N(epsilon)-(carboxymethyl)lysine depositions in intramyocardial blood vessels in human and rat acute myocardial infarction: a predictor or reflection of infarction? *Arterioscler Thromb Vasc Biol*. 2006;26:2497–2503. doi: 10.1161/01.ATV.0000245794.45804.ab
- [4]. Begieneman MP, Van De Goot FR, Krijnen PA, Fritz J, Paulus WJ, Spreeuwenberg MD, Van Hinsbergh VW, Niessen HW. The basement membrane of intramyocardial capillaries is thickened in patients with acute myocardial infarction. *Journal of vascular research*. 2009;47:54–60.
- [5]. Fiet MD, Azouz B, Robbers L, Niessen HWM, Krijnen PAJ. Increased epicardial nerves and decreased intramyocardial PVAT in acute myocardial infarction. *Eur J Clin Invest*. 2023:e14057. doi: 10.1111/eci.14057
- [6]. Vijayan S, S Barmby D, R Pearson I, G Davies A, B Wheatcroft S, Sivananthan M. Assessing coronary blood flow physiology in the cardiac catheterisation laboratory. *Current cardiology reviews*. 2017;13:232–243.
- [7]. Dai Z, Aoki T, Fukumoto Y, Shimokawa H. Coronary perivascular fibrosis is associated with impairment of coronary blood flow in patients with non-ischemic heart failure. *Journal of cardiology*. 2012;60:416–421.
- [8]. Fitzgerald AA, Weiner LM. The role of fibroblast activation protein in health and malignancy. *Cancer Metastasis Rev*. 2020;39:783–803. doi: 10.1007/s10555-020-09909-3
- [9]. Lay AJ, Zhang HE, McCaughan GW, Gorrell MD. Fibroblast activation protein in liver fibrosis. *Front Biosci (Landmark Ed)*. 2019;24:1–17. doi: 10.2741/4706
- [10]. Tillmanns J, Hoffmann D, Habbaba Y, Schmitto JD, Sedding D, Fraccarollo D, Galuppo P, Bauersachs J. Fibroblast activation protein alpha expression identifies activated fibroblasts after myocardial infarction. *J Mol Cell Cardiol*. 2015;87:194–203. doi: 10.1016/j.yjmcc.2015.08.016
- [11]. Zeisberg EM, Tarnavski O, Zeisberg M, Dorfman AL, McMullen JR, Gustafsson E, Chandraker A, Yuan X, Pu WT, Roberts AB. Endothelial-to-mesenchymal transition contributes to cardiac fibrosis. *Nature medicine*. 2007;13:952–961.
- [12]. Hashimoto N, Phan SH, Imaizumi K, Matsuo M, Nakashima H, Kawabe T, Shimokata K, Hasegawa Y. Endothelial-mesenchymal transition in bleomycin-induced pulmonary fibrosis. *American journal of respiratory cell and molecular biology*. 2010;43:161–172.
- [13]. Rensen SSM, Doevendans PAFM, van Eys GJJM. Regulation and characteristics of vascular smooth muscle cell phenotypic diversity. *Netherlands Heart Journal*. 2007;15:100–108. doi: 10.1007/BF03085963
- [14]. Lu S, Jolly AJ, Strand KA, Dubner AM, Mutryn MF, Moulton KS, Nemenoff RA, Majesky MW, Weiser-Evans MC. Smooth muscle-derived progenitor cell myofibroblast differentiation through KLF4 downregulation promotes arterial remodeling and fibrosis. *JCI insight*. 2020;5.
- [15]. Begieneman MP, Emmens RW, Rijvers L, Woudstra L, Paulus WJ, Kubat B, Vonk AB, van Rossum AC, Wouters D, Zeerleder S. Myocardial infarction induces atrial inflammation that can be prevented by C1-esterase inhibitor. *Journal of clinical pathology*. 2016.
- [16]. Garate-Carrillo A, Gonzalez J, Ceballos G, Ramirez-Sanchez I, Villarreal F. Sex related differences in the pathogenesis of organ fibrosis. *Translational Research*. 2020;222:41–55. doi: <https://doi.org/10.1016/j.trsl.2020.03.008>
- [17]. Nosalski R, Siedlinski M, Denby L, McGinnigle E, Nowak M, Cat AND, Medina-Ruiz L, Cantini M, Skiba D, Wilk G, et al. T-Cell-Derived miRNA-214 Mediates Perivascular Fibrosis in Hypertension. *Circ Res*. 2020;126:988–1003. doi: 10.1161/circresaha.119.315428
- [18]. Özkan E, Çetin-Taş Y, Şekerdağ E, Kızılrımk AB, Taş A, Yıldız E, Yapıcı-Eser H, Karahüseyinoğlu S, Zeybel M, Gürsoy-Özdemir Y. Blood-brain barrier leakage and perivascular collagen accumulation precede microvessel rarefaction and memory impairment in a chronic hypertension animal model. *Metab Brain Dis*. 2021;36:2553–2566. doi: 10.1007/s11011-021-00767-8
- [19]. Widyanoro B, Emoto N, Nakayama K, Anggrahini DW, Adiarto S, Iwasa N, Yagi K, Miyagawa K, Rikitake Y, Suzuki T. Endothelial cell-derived endothelin-1 promotes cardiac fibrosis in diabetic hearts

- through stimulation of endothelial-to-mesenchymal transition. *Circulation*. 2010;121:2407–2418.
- [20]. Ytrehus K, Hulot JS, Perrino C, Schiattarella GG, Madonna R. Perivascular fibrosis and the microvasculature of the heart. Still hidden secrets of pathophysiology? *Vascul Pharmacol*. 2018. doi: 10.1016/j.vph.2018.04.007
- [21]. Costa RM, Neves KB, Tostes RC, Lobato NS. Perivascular adipose tissue as a relevant fat depot for cardiovascular risk in obesity. *Frontiers in physiology*. 2018;9:253.
- [22]. Bujak M, Frangogiannis NG. The role of TGF- $\beta$  signaling in myocardial infarction and cardiac remodeling. *Cardiovascular research*. 2007;74:184–195.
- [23]. Ertl G, Frantz S. Healing after myocardial infarction. *Cardiovascular Research*. 2005;66:22–32. doi: 10.1016/j.cardiores.2005.01.011
- [24]. Rosello-Lleti E, Delgado Arija M, Genoves Martinez P, Perez Carrillo L, Gimenez Escamilla I, Gonzalez I, Portoles M, Tarazon E. The central role of FAP dysregulation and cardiac fibroblast activation in heart failure patients. *European Heart Journal*. 2023;44. doi: 10.1093/eurheartj/ehad655.725
- [25]. Aghajanian H, Kimura T, Rurik JG, Hancock AS, Leibowitz MS, Li L, Scholler J, Monslow J, Lo A, Han W, et al. Targeting cardiac fibrosis with engineered T cells. *Nature*. 2019;573:430–433. doi: 10.1038/s41586-019-1546-z
- [26]. Evrard SM, Lecce L, Michelis KC, Nomura-Kitabayashi A, Pandey G, Purushothaman KR, d'Escamard V, Li JR, Hadri L, Fujitani K, et al. Endothelial to mesenchymal transition is common in atherosclerotic lesions and is associated with plaque instability. *Nat Commun*. 2016;7:11853. doi: 10.1038/ncomms11853
- [27]. Wirka RC, Wagh D, Paik DT, Pjanic M, Nguyen T, Miller CL, Kundu R, Nagao M, Collier J, Koyano TK, et al. Atheroprotective roles of smooth muscle cell phenotypic modulation and the TCF21 disease gene as revealed by single-cell analysis. *Nature Medicine*. 2019;25:1280–1289. doi: 10.1038/s41591-019-0512-5
- [28]. Wu J, Saleh MA, Kirabo A, Itani HA, Montaniel KR, Xiao L, Chen W, Mernaugh RL, Cai H, Bernstein KE, et al. Immune activation caused by vascular oxidation promotes fibrosis and hypertension. *J Clin Invest*. 2016;126:50–67. doi: 10.1172/jci80761
- [29]. Welch-Reardon KM, Ehsan SM, Wang K, Wu N, Newman AC, Romero-Lopez M, Fong AH, George SC, Edwards RA, Hughes CC. Angiogenic sprouting is regulated by endothelial cell expression of Slug. *Journal of cell science*. 2014;127:2017–2028.
- [30]. VILLARI B, CAMPBELL SE, SCHNEIDER J, VASSALLI G, CHIARIELLO M, HESS OM. Sex-dependent differences in left ventricular function and structure in chronic pressure overload. *European Heart Journal*. 1995;16:1410–1419. doi: 10.1093/oxfordjournals.eurheartj.a060749